International Conference on Applied Energy 2019
Aug 12-15, 2019, Västerås, Sweden
Paper ID: 72

STRESS MONITORING DURING OPTIMAL DYNAMIC OPERATION OF A NATURAL GAS COMBINED CYCLE: LINEAR VS NONLINEAR FORMULATION

Jairo Rúa*, Lars O. Nord

Department of Energy and Process Engineering, Norwegian University of Science and Technology – NTNU, Trondheim, Norway

ABSTRACT

Natural gas combined cycles are expected to operate in a flexible manner in the future energy markets to complement the increasing variable renewable electricity generation. Stresses in thick-walled components and gas turbine load ramps are the main limitations in the dynamic operation of NGCCs. This work presents two different modelling approaches of the thermal and mechanical stresses originated in the high-pressure drum and steam turbine rotor, and compares four different formulations, two linear and two nonlinear, of the optimization problem included in the model predictive control strategy. A case study shows the capability of the proposed control methodology to optimally operate the NGCC without exceeding the maximum allowable stress in the critical components.

Keywords: gas turbine combined cycle, thermal and mechanical stress, optimal control strategy, flexible thermal power plant, dynamic modelling and simulation, dynamic optimization.

NOMENCLATURE

Abbreviations	
MPC	Model Predictive Control
NGCC	Natural Gas Combined Cycle
Latin Symbols	
E	Young's Modulus
h	Convection coefficient
p	Pressure
r	Radius
T	Temperature deviation from design
Greek Symbols	
α	Thermal expansion coefficient
ω	Rotational speed
ρ	Density
σ	Stress
υ	Poisson's ratio
Subscripts	
θ	Tangential direction
i	Inner radius
o	Outer radius
r	Radial direction
z	Longitudinal direction

1. INTRODUCTION

Flexible operation of thermal power plants will play a key role in future energy markets [1]. The increasing contribution of renewable energy sources, mainly wind solar, to the electric system together with their non-dispatchability will force the traditional thermal power plants to adapt their operation [2]. In this context, natural gas combined cycles are arguably the main complement because of their capacity to rapidly change the power generation while keeping a high efficiency [3].

Gas turbine load ramps and stresses in thick-walled equipment are the main limitation during the transient operation of natural gas combined cycles [4]. Alobaid et al. [5] demonstrated that the start-up time could be reduced if it was possible to guarantee that material limits were not exceeded. Can Gülen and Kim [6] also showed the importance of monitoring the stresses in the high-pressure drum and steam turbine rotor during the start-up of a NGCC, while Shirakawa et al. [7] proved that dynamic optimization of start-up sequences may lead to faster operation without exceeding the maximum allowable stress in critical equipment.

Model predictive control solves a dynamic optimization problem every sampling time. Therefore, its application to control of thermal power with stress monitoring may lead to improvements in their dynamic performance. Prasad et al. [8] already proved the suitability of MPC for stabilizing steam cycles, while Rúa et al. [9] showed how MPC may be utilized to predict the stresses in any equipment of the power plant and hence compute an optimal control sequence that ensures that the maximum stresses in these components are not exceeded. In their work, Rúa et al. [9] developed stress models for the high-pressure drum and the first-stage steam turbine rotor and embedded them in a quadratic programming optimization algorithm together with simplified models of the power plant. Results showed the capability of the proposed control strategy to optimally operate the NGCC without exceed the materials' limits even when tight constraints were imposed.

This works compares two different modelling approaches of the stresses in the high-pressure drum and the first-stage steam turbine rotor, described in Section 2, and four different MPC's optimization problem formulation, two linear and two nonlinear, discussed in Section 3. The accuracy of the two modelling approaches and the performance of four formulations is discussed in Section 4 and a case study analyzing the performance of one of these formulations under highly fluctuating demands is presented to show the optimal control of the proposed methodology. Concluding remarks are summarized in Section 5.

2. MODELLING

2.1 Natural Gas Combined Cycle Detailed Model

A modern three-pressure level natural gas combined cycle with reheating and steam extraction was designed using GT PRO by Thermoflow [10] as it provides detailed information of the equipment's geometry. The dynamic model utilized in this work was developed with the Thermal Power library in the Modelica-based software Dymola. This model is hereafter called the detailed dynamic model.

Steady-state and part-load model to model validation proved the adequacy of the detailed model. A detailed description of the dynamic modelling and validation results can be found in the work of Rubén et al. [11].

2.2 Thermal and Mechanical Stresses

The high-pressure drum and the first stage turbine rotor are critical components where large stresses arise because of the high-pressure steam and the large temperature gradients in their thick walls. Therefore, both are monitored during the transient operation of the power plant to ensure that the maximum allowable stress is not exceeded. The stresses in the drum are modelled by assuming plane strain while plane stress is considered in the rotor [12].

This work proposes two different approaches to model the stresses arising in the walls of this equipment. The first modelling approach combines the constitutive equations, which relate the stress with the strain, with the strain-displacement relations. This allows expressing the stress components in terms of the displacement and the temperature in radial direction. If these equations are inserted in the radial equilibrium equation, a system of differential-algebraic equations relating the temperature in radial direction, the displacement and the stress is obtained [12]. These equations were solved numerically by applying a Crank-Nicholson discretization scheme for the temperature distribution and central finite differences for the displacement and the stresses. This system of equations was developed by Rúa et al. [9] and is presented in the Supplementary Material included therein.

The second approach analytically solves the ordinary differential equation obtained in the previous model in order to eliminate the displacement. The stress components of the drum are:

$$\begin{aligned}\sigma_r = {} & \left(1-\frac{r_i^2}{r^2}\right)\frac{E\alpha}{(1+\upsilon)(1-2\upsilon)}\int_{r_i}^{r_o} rT\ \mathrm{d}r - \frac{E\alpha}{1-\upsilon}\int_{r_i}^{r} rT\ \mathrm{d}r + \\ & + p_o\left[\frac{r_o^2 r_i^2}{(r_o^2-r_i^2)r^2} - \frac{r_o^2}{(r_o^2-r_i^2)}\right] + p_i\left[\frac{r_o^2}{(r_o^2-r_i^2)} - 1 - \frac{r_o^2 r_i^2}{(r_o^2-r_i^2)r^2}\right]\end{aligned} \tag{1}$$

$$\begin{aligned}\sigma_\theta = {} & \left(1+\frac{r_i^2}{r}\right)\frac{E\alpha}{(1-\upsilon)(r_o^2-r_i^2)}\int_{r_i}^{r_o} rT\ \mathrm{d}r + \frac{E\alpha}{1-\upsilon}\left(\frac{1}{r^2}\int_{r_i}^{r} rT\ \mathrm{d}r - T\right) + \\ & + p_i\left[\frac{r_o^2}{r_o^2-r_i^2} - 1 + \frac{r_o^2 r_i^2}{(r_o^2-r_i^2)r^2}\right] - p_o\left[\frac{r_o^2}{r_o^2-r_i^2} + \frac{r_o^2 r_i^2}{(r_o^2-r_i^2)r^2}\right]\end{aligned} \tag{2}$$

$$\begin{aligned}\sigma_z = {} & \frac{2\upsilon E\alpha}{(r_o^2-r_o^2)(1-\upsilon)}\int_{r_i}^{r_o} rT\,\mathrm{d}r - \frac{E\alpha}{1-\upsilon}T + \\ & + p_i\left(\frac{2\upsilon r_o^2}{r_o^2-r_i^2} - 2\upsilon\right) - p_o\,\frac{2\upsilon r_o^2}{r_o^2-r_i^2}\end{aligned} \tag{3}$$

Table 1: Validation boundary conditions.

Component	Thermal Boundary Conditions				Mechanical Boundary Conditions		Rotation
	$T_{initial}$	Ramp	h_i	h_o	r_i	r_o	
Drum	340 [°C]	± 20	20000 [W/m^2 °C]	0.065 [W/m^2 °C]	p = 150 [bar]	p = 1 [bar]	-
Rotor	590 [°C]	± 10	-	20000 [W/m^2 °C]	u = 0 [m]	p = 140 [bar]	3000 [rpm]

The rotor stress components are defined as:

$$\begin{aligned}\sigma_r = &-\frac{E\,\alpha}{r^2}\int_{r_i}^{r} rT\,\mathrm{d}r + \frac{\rho\,\omega^2}{8}\left[(1+\upsilon)\,r_i^2-(3+\upsilon)\,r^2\right]+\\ &\left[1+\upsilon+\frac{(1-\upsilon)r_i^2}{r^2}\right]\frac{r_o^2}{(1+\upsilon)r_o^2+(1-\upsilon)r_i^2}\left(\frac{E\alpha}{r_o^2}\int_{r_i}^{r_o} rT\,\mathrm{d}r-p_o\right)+\\ &+\frac{\rho\omega^2 r_o^2(1+\upsilon)}{8\left[(1+\upsilon)r_o^2+(1-\upsilon)r_i^2\right]}\left[r_o^2(3+\upsilon)-r_i^2(1+\upsilon)\right]+\\ &+\frac{\rho\omega^2 r_o^2 r_i^2(1-\upsilon)}{8r^2\left[(1+\upsilon)r_o^2+(1-\upsilon)r_i^2\right]}\left[r_o^2(3+\upsilon)-r_i^2(1+\upsilon)\right]\end{aligned} \tag{4}$$

$$\begin{aligned}\sigma_\theta = &E\,\alpha\left(\frac{1}{r^2}\int_{r_i}^{r_o} rT\,\mathrm{d}r - T\right)+\frac{\rho\,\omega^2}{8}\left[(1+\upsilon)r_i^2-(1+3\upsilon)r^2\right]+\\ &+\left[1+\upsilon-\frac{(1-\upsilon)r_i^2}{r^2}\right]\frac{r_o^2}{(1+\upsilon)r_o^2+(1-\upsilon)r_i^2}\left(\frac{E\alpha}{r_o^2}\int_{r_i}^{r_o} rT\,\mathrm{d}r-p_o\right)+\\ &+\frac{\rho\,\omega^2(1+\upsilon)\,r_o^2}{8\left[(1+\upsilon)r_o^2+(1-\upsilon)r_i^2\right]}\left[r_o^2(3+\upsilon)-r_i^2(1+\upsilon)\right]+\\ &+\frac{\rho\,\omega^2(1-\upsilon)\,r_o^2 r_i^2}{8r^2\left[(1+\upsilon)r_o^2+(1-\upsilon)r_i^2\right]}\left[r_i^2(1+\upsilon)-r_o^2(3+\upsilon)\right]\end{aligned} \tag{5}$$

These equations were expressed as a linear system of equations by applying the trapezoidal rule to the integrals in Eqs.(1)-(5). Validation of the models proposed in both approaches was carried out with the specialized software ANSYS. Table 1 summarizes the boundary conditions imposed during the validation, and Figure 1 and 2 represent the comparison among the different models.

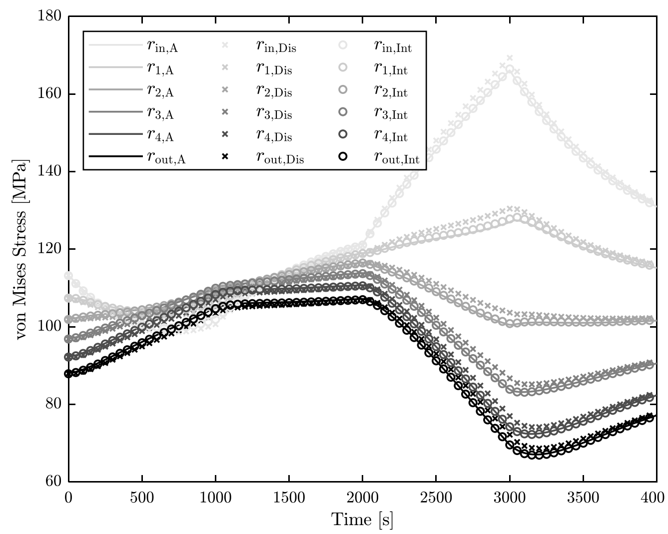

Figure 1: von Mises equivalent stress along six equidistant radii in the drum. A refers to Ansys, Dis to displacement and Int to integrals.

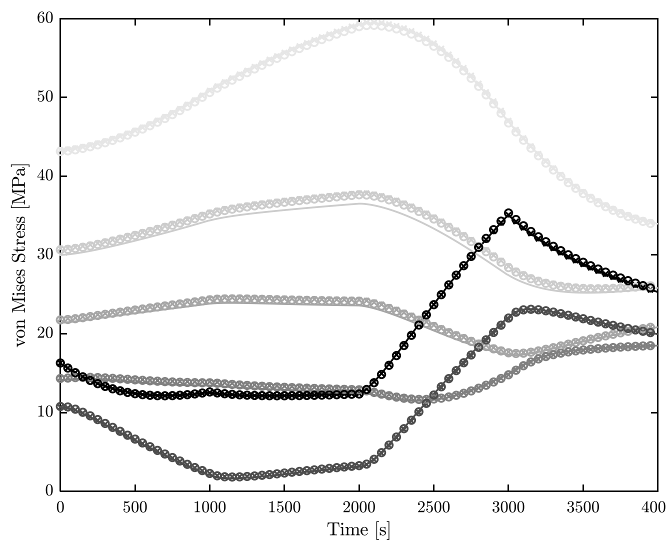

Figure 2: von Mises equivalent stress along six equidistant radii in the rotor. Same legend as in the drum validation results.

2.3 Simplified Models

Model predictive control requires solving a dynamic optimization problem every sampling time. As the dominant dynamic of the system occur in approximately 300 seconds, a sampling time of 30 seconds was selected. Therefore, to carry out the optimization within this time interval, simplified models predicting key thermodynamic variables of the power plant are required.

System identification [13] was utilized to generate these simplified models based on data obtained from simulations of the detailed dynamic model. Linear polynomials and Autoregressive Exogenous variable (ARX) models interpolated with a Gaussian validation function were fitted to this data by minimizing the error between their prediction and the set of data. A detailed description of these simplified models and their validation can be found in the work of Rúa et al. [9].

3. CONTROL STRATEGY

Model predictive control relies on the solution of a dynamic optimization problem every sampling time. The stress and simplified models enter the optimization problem as equality constraints, lower and upper boundaries are imposed on the optimization variables, and an inequality constraint in the maximum gas turbine load ramp is included. This control aims at minimizing the difference between the power generation and demand, and the fluctuation of the superheat and reheat steam temperature.

Both linear and nonlinear formulations of the optimization problem for the two different stress models are compared in this work. The simplified models are always embedded as linear equality constraints, while the stress models enter as linear or nonlinear equality constraints depending on the formulation. In the nonlinear approach, the stress model and the von Mises effective stress are included as nonlinear equality and inequality constraints, respectively, while in the linear MPC a linearization of the von Mises stress expression is required to enter the formulation as a linear constraint.

The difference between these two formulations lies in how the stress models of the drum and the rotor are evaluated. In the linear approach the stress model variables are also optimization variables modified simultaneously with the degrees of freedom. The nonlinear MPC only uses the simplified model variables as optimization variables at the expense of having to evaluate the stress models separately to check that the constraints are not violated. Details of the linear MPC formulation with the displacement stress model are included in the work of Rúa et al [9].

4. RESULTS AND DISCUSSION

4.1 Computational Time Analysis

As computational time is an important limitation for the MPC strategies, a comparison among the required times to compute an optimal control sequence of the different formulations is carried out. Table 2 includes the computational time relative to the fastest formulation.

Linear MPC shows superior performance of the stress model. Despite the fewer optimization variables in the nonlinear formulation, the evaluation of the stress model as a nonlinear constraint requires more time, leading to longer computational times. The integral-based model where the displacement is not computed seems to generate slightly faster optimizations. However, this is difficult to evaluate since each stress model requires different spatial discretizations and different values may lead to similar computational times. Therefore, both stress models are suitable for their implementation in the proposed control strategy in terms of both accuracy and computational performance.

Table 2: Relative computational time for the different MPC formulations. Dis refers to displacement and Int to integrals.

Formulation	Linear		Nonlinear	
Stress Model	Dis	Int	Dis	Int
Relative Time	1.88	1	41.02	27.19

4.2 Case Study

To prove the robustness of the proposed control methodology, a tight constraint of 125 MPa in the maximum allowable equivalent stress in the high-pressure steam drum was imposed in the linear MPC algorithm during a load step change. Figure 3 and 2 show how the control strategy is able to reach steady-state power generation despite the limitation on the drum's stress.

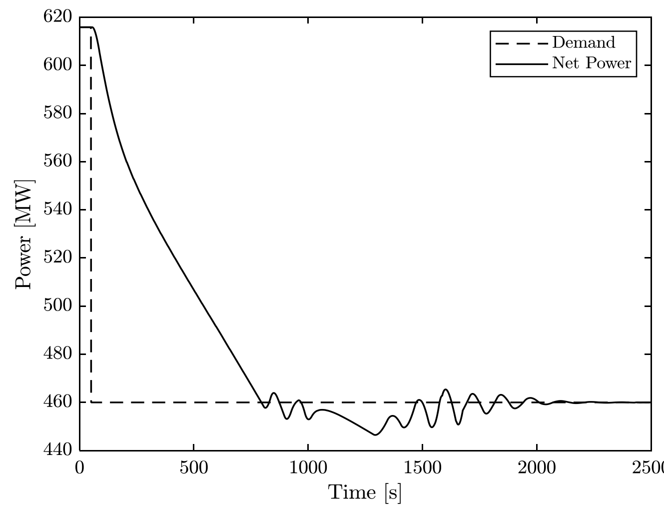

Figure 3: NGCC net power generation.

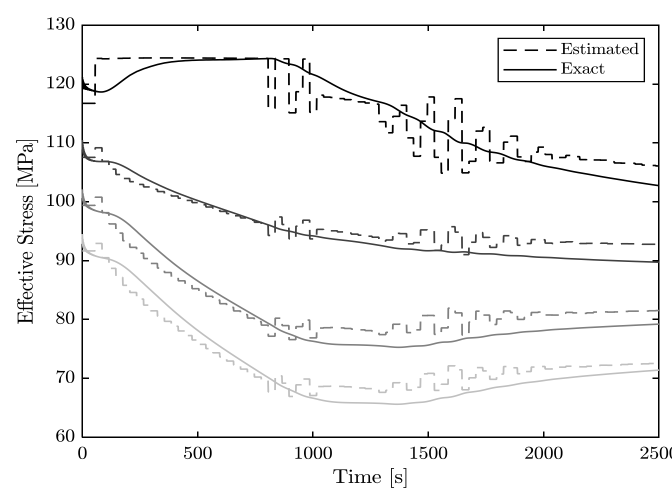

Figure 4: Comparison between the estimated and exact equivalent stress at four equidistant radii.

Figure 4 shows that the constraint in the maximum effective stress in the high-pressure drum is the limiting factor in the power ramp of the NGCC as it is active during almost 1000 seconds. This proves the capability of the stress models and the proposed control strategy to predict and limit the stress in critical equipment while computing the optimal power ramps in the thermal power plant.

Fluctuations in the power generation are a consequence of the tight constraint in the effective stress, the simplified models and the variability of the estimated effective stress. Despite that the simplified models over-predict the dynamic response of certain thermodynamic variables, this variability is mainly originated by the lack of an exact temperature profile in the drum's wall model in the detailed dynamic power plant model, which forces the continuous estimation of wall temperatures that lead to more inaccurate and less stable results. Nevertheless, the estimated effective stress is in good agreement with the exact stress and it avoids that the maximum allowable value is exceeded.

5. CONCLUSIONS

This work presents a control strategy capable of predicting the stresses in critical equipment while computing optimal control sequences that satisfy operational constraints. This control strategy proved its capability to adequality compute optimal control actions without exceeding the imposed constraints. Linear and nonlinear MPC formulations were also compared, showing the superior computational performance of linear MPC. Nonlinear MPC proved to be considerably slower because of the high computational cost of evaluating the stress models during the optimization. Two stress modelling approaches were also compared. Both can accurately predict the stress in the wall of thick-wall equipment while none of them showed to be superior from a computational perspective due to the sensitivity of the number of spatial discretizations. Therefore, both are considered suitable for implementation in the proposed control methodology.

ACKNOWLEDGEMENT

This work has been financially supported by the Department of Energy and Process Engineering at the Norwegian University of Science and Technology - NTNU. The authors thank Dr. Rubén Mocholí Montañés for providing the dynamic model of the power plant.

REFERENCE

[1] Montañés RM, Korpås M, Nord LO, Jaehnert S. Identifying operational requirements for flexible CCS power plant in future energy systems. Energy Procedia. 2016;86:22-31.

[2] Eser P, Chokani N, Abhari RS. Operational and financial performance of fossil fuel power plants within a high renewable energy mix. Journal of the Global Power and Propulsion Society. 2017;1:16-27.

[3] Gonzalez-Salazar MA, Kirsten T, Prchlik L. Review of the operational flexibility and emissions of gas-and coal-fired power plants in a future with growing renewables. Renewable and Sustainable Energy Reviews. 2018;82:1497-513.

[4] Alobaid F, Mertens N, Starkloff R, Lanz T, Heinze C, Epple B. Progress in dynamic simulation of thermal power plants. Progress in energy and combustion science. 2017;59:79-162.

[5] Alobaid F, Postler R, Ströhle J, Epple B, Kim H-G. Modeling and investigation start-up procedures of a combined cycle power plant. Applied Energy. 2008;85:1173-89.

[6] Gülen SC, Kim K. Gas Turbine combined cycle dynamic simulation: a physics based simple approach. Journal of Engineering for Gas Turbines and Power. 2014;136:011601.

[7] Shirakawa M, Nakamoto M, Hosaka S. Dynamic simulation and optimization of start-up processes in combined cycle power plants. JSME International Journal Series B Fluids and Thermal Engineering. 2005;48:122-8.

[8] Prasad G, Swidenbank E, Hogg B. A local model networks based multivariable long-range predictive control strategy for thermal power plants. Automatica. 1998;34:1185-204.

[9] Rúa J, Agromayor R, Hillestad M, Nord LO. Optimal Dynamic Operation of Natural Gas Combined Cycles Accounting for Stresses in Thick-Walled Components. Applied Energy. 2019;Submitted.

[10] GT PRO 24.0. Thermoflow Inc. 2014.

[11] Montañés RM, GarÐarsdóttir SÓ, Normann F, Johnsson F, Nord LO. Demonstrating load-change transient performance of a commercial-scale natural gas combined cycle power plant with post-combustion CO2 capture. International Journal of Greenhouse Gas Control. 2017;63:158-74.

[12] Timoshenko S, Goodier N. Theory of Elasticity: McGraw-Hill, New York, NY; 1951.

[13] Ljung L. System Identification: Theory for the User. Prentice Hall Information and System Sciences Serie (T. Kailath, ed.). Englewood Cli s, NJ. 1987.

